JOURNAL OF GUIDANCE, CONTROL, AND DYNAMICS
Vol. 16, No. 3, May-June 1993

Sensor Failure Detection and Isolation in Flexible Structures Using System Realization Redundancy

David C. Zimmerman* and Terri L. Lyde†
University of Florida, Gainesville, Florida 32611

Sensor failure detection and isolation for flexible structures is approached from a system realization perspective. Instead of using hardware or analytical model redundancy, system realization is utilized to provide an experimental based model redundancy. The failure detection and isolation algorithm utilizes the eigensystem realization algorithm to determine a minimum-order state-space realization of the structure in the presence of noisy measurements. The failure detection and isolation algorithm utilizes statistical comparisons of successive realizations to detect and isolate the failed sensor component. Because of the nature in which the failure detection and isolation algorithm is formulated, it is also possible to classify the failure mode of the sensor. Results are presented using both numerically simulated and actual experimental data.

I. Introduction

THE design, control, and maintenance of future large space structures (LSS) offers many new and different challenges for engineers. The economic requirement of lightweight structures coupled with the large physical dimensions needed to meet mission objectives necessitates the use of active vibration control. The large number of actuators and sensors required for precise control of LSS together with the desire for long periods of operation between maintenance periods brings about the need for a reliable monitoring system to detect actuator and sensor failures. It can easily be shown that in a typical large space structure control system with 400 components, each with an exponential distribution of time to failure with a mean time to failure of 100,000 h, one can expect a component failure every 10 days. In this paper, an algorithm to detect, isolate, and classify sensor failures for flexible structure control systems is presented.

During the last three decades, many researchers have addressed the development of failure detection and isolation algorithms.[1,2] References 1 and 2 provide extensive surveys of various approaches. Early fault detection schemes were based on hardware redundancy. Hardware redundancy schemes use three (or more) sensors for each physical quantity that is to be measured. The multiple sensor outputs are then compared at regular time intervals. A sensor output not agreeing completely with the other two is then flagged as being faulty. For LSS, the high cost of both space qualified hardware as well as launch costs may make hardware duplication infeasible.

More recent schemes are based on analytical redundancy that eliminates the need for extra hardware. Analytical redundancy implies the use of an analytically developed mathematical model to analytically generate signals that would otherwise be produced by redundant hardware. These functionally redundant schemes employ state estimation, parameter estimation, adaptive filtering, variable threshold logic, statistical decision theory and various combinatorial and logical operations. The differences between the sensor signals and the analytical redundancy produced signals are then used to define an error residual. Inspection of this residual is then used to detect and isolate failures.

There have been a number of application studies of failure detection and isolation (FDI) techniques including some actual applications to either process plants or laboratory experiments using real time equipment. As a few examples, Watanabe and Himmelblau[3] demonstrated fault detection strategies for nonlinear chemical reactors. Shiozaki et al.[4] diagnosed faults in pipeline systems using signed directional graphs. Kerr[5] used Kalman filters to detect faults in inertial navigation systems. Deckert et al.[6] used Kalman filters for fault identification on the NASA F8 digital fly-by-wire aircraft. Finally, Baruh and Choe[7] and VanderVelde[8] have investigated FDI systems in the context of flexible structures.

Along with the many different areas of applications for fault detection systems comes many different techniques. Beard[9] proposed a failure detection filter in conjunction with methods of self-reorganization to maintain closed-loop stability. The failure detection filter is functionally the same as a Kalman filter, except that the gain matrix is designed to restrict the residual signature of a failed sensor to a two-dimensional subspace of the residual space. Mehra and Peschon[10] introduced a general procedure for FDI in dynamic systems with the aid of a single Kalman filter. An innovation sequence was generated and subjected to statistical tests of whiteness, mean, and covariance. Knowing the time histories of the output variables under normal conditions, the deviations under faulty conditions are detected by statistical decision theory. Montgomery and Caglayan[11] proposed the Bayesian decision theory which uses several Kalman filters. A bank of m parallel Kalman filters designed for a set of $m-1$ possible failure modes is used with hypothesis testing to detect failures. Deckert et al.[6] describe a functional redundancy scheme combined with dual sensor redundancy of the process. Failure identification is accomplished on the basis of the functional relationships among the outputs of dissimilar instruments by performing sequential probability ratio tests of the differences among the outputs. A similar concept called the generalized likelihood test was proposed by Daly et al.[12] Several contributions to FDI with state estimation methods using either observers or Kalman filters were made by Clark.[13] The dedicated observer scheme (DOS) of Clark utilizes a bank of Luenberger observers, each driven by one sensor output. If none of the sensors fails, all of the reconstructed state vectors converge to the actual state vector. If one of the sensors fails, then a difference occurs in the output vector of the corresponding observer. This can be used to identify the faulty sensor. To handle the FDI problem in the presence of random disturbances, Clark and Campbell[14] modified the DOS scheme by

Received Aug. 9, 1991; revision received May 25, 1992; accepted for publication July 24, 1992.

*Associate Professor, Department of Aerospace Engineering, Mechanics, and Engineering Sciences. Member AIAA.

†Graduate Student, Department of Aerospace Engineering, Mechanics, and Engineering Sciences; currently Subsystem Engineer, Lockheed Corporation, Marietta, Georgia.

using a dedicated Kalman filter for each of the sensors, but instead of driving each filter by a single sensor output, it is driven by three sensors where each filter is sensitized to faults in a single sensor.

In the FDI schemes described so far, the errors of the reconstructed states that are employed for FDI are affected by both sensor malfunctions and variations of the process parameters. Insensitivity to parameter variations as a design specification was included in the observer design by Frank and Keller.[15] They extended the DOS by duplicating the observers to allow distinction between parameter variations and instrument malfunctions. Several other approaches to the robustness problem were proposed by Belkoura,[16] and Frank and Keller.[17] A general approach of creating robustness in FDI systems has been pursued over the years by Chow and Willsky,[18] Lou et al.,[19] and many others. They look to the problem of robust residual generation from the viewpoint of analytical redundancy relations, and have introduced the concept of general parity checks.

In this paper, a failure detection, isolation and classification algorithm is developed for LSS. The algorithm makes use of system realizations obtained from the eigensystem realization algorithm (ERA).[20] It is assumed that a nominal realization for the LSS is obtained before any sensor failure has occurred. The FDI algorithm is based on comparing future realizations of the LSS to the nominal case.

II. Problem Formulation

A. Structural Formulation

Consider an n-DOF structural model with feedback control,

$$M\ddot{w} + D\dot{w} + Kw = B_0 u \tag{1}$$

where M, D, and K are the $n \times n$ analytical mass, damping, and stiffness matrices, w is an $n \times 1$ vector of positions, B_0 is the $n \times m$ actuator influence matrix; u is the $m \times 1$ vector of control forces; and the overdots represent differentiation with respect to time. This second-order model can be recast in first-order state space form as

$$\dot{x} = \bar{A}x + \bar{B}u \tag{2}$$

where $\bar{A}$ is referred to as the state matrix, and $\bar{B}$ is referred to as the control influence matrix,

$$\bar{A} = \begin{bmatrix} 0 & I \\ -M^{-1}K & -M^{-1}D \end{bmatrix} \qquad \bar{B} = \begin{bmatrix} 0 \\ M^{-1}B_0 \end{bmatrix}$$

In addition, the $r \times 1$ output vector y of sensor measurements is given by,

$$y = Cx \tag{3}$$

where C is the output influence matrix.

Equations (2) and (3) constitute the continuous time model for the flexible structure. Similarly, the structure can be modeled in discrete time form as

$$x(k+1) = Ax(k) + Bu(k) \tag{4}$$

$$y(k) = Cx(k) \tag{5}$$

where A and B are defined as

$$A = e^{\bar{A}\Delta t} \qquad B = e^{\bar{A}2\Delta t}\int_0^{\Delta t} e^{-\bar{A}\zeta}\mathrm{d}\zeta\bar{B} \tag{6}$$

where Δt is the discrete time step.

The triplet of constant matrices $[A, B, C]$ is termed a realization of the structure. Given the structure realization, one can determine the response to any known input. It should be noted that any system has an infinite number of realizations that will predict the identical response to any input. To see this, define a coordinate transformation as

$$x = Tz \tag{7}$$

Substitution of Eq. (7) into Eqs. (4) and (5) yields

$$z(k+1) = T^{-1}ATz(k) + T^{-1}Bu(k) \tag{8}$$

$$y(k) = CTz(k) \tag{9}$$

The effect of input $u(k)$ on output $y(k)$ will be the same whether Eqs. (4) and (5) or Eqs. (8) and (9) are used. Thus, the triple $[T^{-1}AT, T^{-1}B, CT] = [A', B', C']$ is also a realization for the structure.

B. System Realization

For the FDI algorithm proposed, the eigensystem realization algorithm (ERA) is utilized to determine the structure realization.[20] ERA is an extension of minimum realization theory[21] to handle the case of noisy measurement data. A unique approach based on a generalized Hankel matrix is used in conjunction with the singular value decomposition to arrive at a minimum-order state-space realization which preserves input-output characteristics. Thus, the output of ERA is the matrix triple $[T^{-1}AT, T^{-1}B, CT] = [A', B', C']$. The Hankel matrix is obtained from the impulse response of the structure. The impulse response may be obtained from an impulse response test of the structure or by taking the inverse fast Fourier transform (FFT) of the frequency response functions measured from a broadband forced test of the structure.

There are a vast number of different system realization algorithms and approaches reported on in the literature. An extensive pre-1986 bibliography of realization theory approaches provided in Ref. 22 contains 143 entries. Several realization approaches have focused on structural system identification, including ERA,[20] ERA with Data Correlation (ERA-DC),[23] Q-Markov cover,[24] and an algorithm due to Moonen et al.[25] A comprehensive review of these algorithms can be found in Ref. 26. Any of these algorithms could be used within the FDI algorithm described subsequently. It would be anticipated that the choice of which realization technique to use in the FDI algorithm would be strongly guided by the particular structure/sensor system to be monitored. Variables to be considered include anticipated noise level of sensors, ambient disturbance/excitation characteristics, real-time considerations, and structural modal complexity. The purpose of the current paper is to describe the generic development of a realization-based FDI algorithm, not the development for a specific system. Therefore, the choice of using ERA as the realization technique was made as a matter of convenience.

C. Sensor Failure Detection and Isolation

The method proposed to detect sensor failures is based on the comparison of two realizations for the same system. If $\{A_i, B_i, C_i, i = 1, 2\}$ are two minimal realizations of the same system, then there exists a unique invertible matrix T such that[27]

$$A_2 = T^{-1}A_1T \qquad B_2 = T^{-1}B_1 \qquad C_2 = C_1T \tag{10}$$

Furthermore, T can be specified as

$$T = W_1W_2^T(W_2W_2^T)^{-1} \tag{11}$$

or

$$T = [(V_2^TV_2)^{-1}V_2^TV_1]^{-1} \tag{12}$$

where W_i and V_i are the controllability and observability matrices for each system given as

$$V_i = \begin{bmatrix} C_i \\ C_iA_i^1 \\ \cdots \\ C_iA_i^{2n-1} \end{bmatrix} \qquad W_i = [B_i\ A_i^1B_i \cdots A_i^{2n-1}B_i] \tag{13}$$

The approach of the proposed fault detection and isolation algorithm is to detect failures by comparing the two realizations. One realization in the comparison will be defined as the nominal case, the realization before any sensor has failed. The other realizations will be compared to this one. To determine whether or not a sensor failure has occurred, the output influence matrix will be examined.

If $[A_n, B_n, C_n]$ is the nominal realization for the structure and $[A_1, B_1, C_1]$ is another realization, then from Eq. (10)

$$C_n = C_1T \tag{14}$$

As with all systems, noise will be present and a fully populated error matrix E can be defined as

$$E = C_n - C_1T \tag{15}$$

When a sensor fails, it would be expected that one of the rows of E will be greater in magnitude than the others. By comparing the magnitude of the error of each row, the sensor failure can be isolated. Seven failure criteria are used to isolate the failed sensor

$$F_1 = \text{rmean [abs}(E)] \tag{16a}$$

$$F_2 = \text{rmean } (E) \tag{16b}$$

$$F_3 = \text{rnorm } (E) \tag{16c}$$

$$F_4 = \frac{F_1}{\text{rmean [abs } (C_n)]} \tag{16d}$$

$$F_5 = \frac{F_2}{\text{rmean } (C_n)} \tag{16e}$$

$$F_6 = \frac{F_3}{\text{rnorm } (C_n)} \tag{16f}$$

$$F_7 = \sum_{i=1}^{6} \frac{\bar{F}_i}{6} \tag{16g}$$

where the rmean operator is the average of each row, the rnorm operator is the 2-norm of each row, abs is the absolute value operator, and $\bar{F}_i$ is F_i normalized to the unit largest component. The element location corresponding to the largest value of F_i indicates which sensor has failed. The failure criteria F_7 is a composite of the other six failure criteria.

In the case that the Hankel matrix is determined from an impact test, the FDI algorithm must account for the possibility that impacts of different magnitude are used. The difference in magnitude can be approximated by comparing the element by element ratio of C_1T to C_n. This matrix is referred to as the scale factor matrix. In determining the magnitude difference, the most dissimilar row of the ratio matrix is ignored because the failed sensor will not provide correct scale factor information. The dissimilar row is chosen as the row whose row mean differs from the matrix mean to the greatest extent.

In addition, the noise floor of the sensor/structure system must be determined before any failure has occurred. As stated earlier, the error matrix E will always be nonzero even when there is no actual sensor failure if there is any noise present in the system. Thus, a noise floor for the matrix E must be determined so that the case of no sensor failure can also be determined from inspecting the error matrix. This noise floor can be determined by applying the FDI algorithm several times before any sensor fails.

In inspecting the F_i for its largest element, there is the tacit assumption that the FDI algorithm is being applied at frequent intervals so that the possibility of multiple sensor failures is minimized. However, it should be noted that the FDI algorithm can be used to detect multiple sensor failures in a sequential manner. After the first application of the FDI algorithm, the faulty sensor is identified and the time history associated with the sensor can be deleted. The algorithm can then be repeated using the data from the remaining sensors. If there was only a single sensor failure, the resulting error matrix would be within the noise floor of the sensor/structure system. However, if there were multiple failures, another failed sensor could be identified. This process could be repeated until the error matrix is within the noise floor.

D. Failure Classification

Because of the nature in which failures are being detected, it is possible to classify some of the types of failures that will occur by inspecting the error matrix E and the scale factor matrix. In this FDI algorithm, the sensor failure is classified as one of four sensor failure classes: complete sensor failure (no output), gain error failure, random signal output failure, and state correlated failure. Each of these different types of failures show up in the realization in a different manner, as will be demonstrated in the examples. In this section, each failure mode is described and techniques for determining from the FDI algorithm the class of sensor failure is discussed.

Complete sensor failure is the case when the output from the sensor is identically zero

$$y_{if} = 0 + \text{noise} \tag{17}$$

where y_{if} is the output of the ith sensor in a failed mode. In this case, there is no corruption of the ERA identified eigenvalues by the output of the faulty sensor. If the measured data is noise free, the row of the identified C matrix corresponding to the failed sensor will be identically zero. With noise present, the mean of the row will be statistically close to zero. Thus, once the FDI algorithm isolates the faulty sensor, the row mean of the C matrix is examined to check for the zero output condition. This classification can also be verified by checking the element by element inverse of the scale factor matrix. In this matrix, each element in the faulty row is being divided by a small number (in the no-noise case by zero). Thus, the magnitude of each element of the row corresponding to the failed sensor will be much greater than the other rows.

A gain failure is when the sensor outputs the correct waveform, except that it has been scaled by a constant scalar factor α

$$y_{if} = \alpha y_i + \text{noise} \qquad 0 < \alpha < \infty \tag{18}$$

In the noise-free case, there is no effect of the gain failure on the ERA identified eigenvalues. The FDI algorithm calculates the mean and standard deviation of the row elements of the scale factor matrix corresponding to the failed sensor. In the no-noise case, these elements would all be equal to one another. The FDI algorithm classifies the failure as a gain failure when the standard deviation is less than 10% of the mean. The value of 10% is an arbitrary setting that should be adjusted based on the noise floor level and the particular structure of interest.

Random noise failure is the case where the sensor outputs a random time series

$$y_{if} = \text{noise} \tag{19}$$

where it is assumed that the noise has zero mean. In this case, the ERA identified eigenvalues are effected; to what degree is dependent on the level of the noise in comparison to the level

of the other sensors. Thus, a random signal failure is flagged when a large shift in the ERA identified eigenvalues is observed.

Finally, a state-correlated failure is one in which the sensor output is dependent on the state vector

$$y_{if} = \boldsymbol{h}^T \boldsymbol{x} + \text{noise} \tag{20}$$

where $\boldsymbol{h}$ is a vector of constants. Again, in the noise-free case there is no effect of a state-correlated failure on the ERA identified eigenvalues. If the FDI algorithm cannot classify the failure as any of the other previously discussed failure modes, it defaults to a state correlated failure. In essence, the zero output and gain failures are just special cases of a state correlated failure. In the zero output case, the $\boldsymbol{h}$ vector is identically zero. In the gain failure case, the $\boldsymbol{h}$ vector would differ from the correct $\boldsymbol{h}$ vector by a constant factor.

III. Examples

Two examples are provided. One consists of a system where the experimental data is "simulated" using a numerical simulation. The second example consists of a laboratory demonstration of the algorithm.

A. Example 1: Four-Degree-of-Freedom Structural Mode

In this first example, a four-degree-of-freedom structure as shown in Fig. 1 is used as a test bed. The nondimensional mass, stiffness, and damping constants are given as $m = 1$, $k = 5$, and $c = 2$. It is assumed that each structural displacement is measured. This model is used to generate time histories for input to the FDI algorithm. To better simulate a real world environment, a random noise signal is added to the output of each sensor. Table 1 provides a summary of each "numerical experiment" performed. The sampling time for each experiment is 0.10 s.

The nominal case was excited with a unit impulse and had no noise added. The eigenvalues for the system determined by ERA are shown in Table 1.

The first experiment is used to establish the noise floor of the system. The peak noise level on each sensor was taken to be some fixed percentage of the peak level of the true signal output on a sensor by sensor basis. The data in the first experiment was corrupted with 15% noise and there was no sensor failure. The difference in impulse magnitude was accounted for using the scale factor matrix. The 2-norm of the error matrix was 0.0132. The ratio of the 2-norm of the error matrix to the 2-norm of C_n was 0.0510. Several other "noisy" test cases were run with lower levels of noise; each resulted in error norms lower than the 15% noise case. Thus, any realization with norms less than the cited norms will be classified as no failure.

Experiment 2 illustrates the case in which there is no sensor failure. The output time histories are corrupted with 2.5% noise. The scale factor (SF) matrix is given as

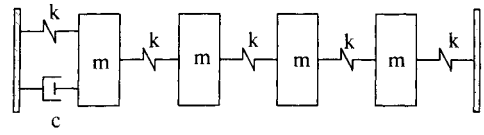

Fig. 1 Four-degree-of-freedom structure test case.

Table 1 Summary of numerical experiments

Experiment No.	Noise, %	Force applied	ERA eigenvalues	Failure type	Failure detected
Nominal	0	Impulse mag = 1	$-0.13+1.42i$ $-0.46+2.70i$ $-0.34+3.40i$ $-0.06+4.18i$	—	—
1	15	Impulse mag = 3	$-0.13+1.42i$ $-0.46+2.71i$ $-0.34+3.40i$ $-0.06+4.18i$	—	—
2	2.5	Impulse mag = 1	$-0.13+1.42i$ $-0.48+2.70i$ $-0.33+3.40i$ $-0.06+4.18i$	None	None
3	0	Impulse mag = 1	$-0.13+1.42i$ $-0.46+2.70i$ $-0.34+3.40i$ $-0.06+4.18i$	No output sensor 1	No output sensor 1
4	2.5	Impulse mag = 2	$-0.15+1.38i$ $-0.43+3.12i$ $-0.41+4.33i$ $-1.92+31.4i$	Random sensor 4	Random sensor 4
5	5	Impulse mag = 1	$-0.00+1.00i$ $-0.10+1.42i$ $-0.23+3.11i$ $-0.01+4.14i$	Sine sensor 3	Random sensor 3
6	7	Impulse mag = 3.5	$-0.13+1.42i$ $-0.47+2.70i$ $-0.35+3.39i$ $-0.07+4.18i$	Random sensor 2	Correlated sensor 2
7	10	Impulse mag = 1.4	$-0.14+1.42i$ $-0.47+2.71i$ $-0.37+3.41i$ $-0.07+4.17i$	Gain sensor 3	Gain sensor 3
8	5	Impulse mag = 1	$-0.14+1.42i$ $-0.50+2.71i$ $-0.38+3.38i$ $-0.07+4.17i$	Correlated sensor 1	Correlated sensor 1

$$\text{SF} = \begin{bmatrix} 1.006 & 0.996 & 1.007 & 1.012 & 0.997 & 1.003 & 0.991 & 1.038 \\ 0.999 & 0.997 & 0.996 & 0.995 & 0.978 & 0.991 & 0.952 & 0.942 \\ 1.002 & 1.001 & 1.019 & 0.990 & 1.003 & 0.996 & 1.023 & 1.060 \\ 1.002 & 0.994 & 0.996 & 1.024 & 1.006 & 1.015 & 1.333 & 0.956 \end{bmatrix}$$

The fourth row is determined to be the most dissimilar; the resulting scale factor is determined to be 0.9997. The FDI algorithm then compensates for the magnitude difference by dividing $C_1 T$ by the scale factor. The error matrix is calculated to be

$$E = 10^{-3} * \begin{bmatrix} -0.241 & 0.291 & 0.137 & 0.395 & -0.060 & 0.176 & 0.952 & 1.035 \\ 0.989 & 0.254 & -0.069 & 0.485 & -0.637 & 0.757 & -0.609 & 0.465 \\ -0.233 & -0.106 & 0.919 & -0.457 & 0.110 & -0.235 & 0.374 & -0.463 \\ -0.134 & 0.457 & 0.346 & 0.265 & -0.485 & 0.150 & 0.365 & 0.372 \end{bmatrix}$$

The 2-norm of the error matrix and the ratio of the 2-norm of the error matrix to the 2-norm of C_n is 0.0018 and 0.0069, respectively. Since these are below the noise threshold, the FDI algorithm correctly concludes that there is no sensor failure.

For the remaining experiments, the error norms were all greater than the established noise floor and will not be reported. The results of the seven failure criteria applied to the remaining numerical experiments are summarized in Table 2. Further discussion on the numerical experiments follow.

Experiment 3 illustrates the case when a sensor is dead, i.e., the sensor has no output. The output data was not corrupted with noise. The scale factor is calculated to be 0.9977 and the realized/transformed output influence matrix is calculated to be

$$C_1T = \begin{bmatrix} 0.000 & 0.000 & 0.000 & 0.000 & 0.000 & 0.000 & 0.000 & 0.000 \\ 0.107 & 0.103 & -0.021 & 0.097 & -0.029 & 0.090 & -0.012 & 0.008 \\ 0.096 & 0.129 & -0.048 & -0.048 & -0.036 & -0.068 & -0.016 & 0.008 \\ 0.058 & 0.084 & 0.100 & -0.011 & 0.081 & -0.010 & -0.001 & 0.009 \end{bmatrix}$$

When the sensor has no output, the row corresponding to that sensor in the realized output influence matrix will have a row mean close to zero. This is used to classify the failure as sensor 1 failing with no output.

Experiment 4 illustrates the case when a sensor outputs a random signal. The rms value of the random signal was chosen to be the same order of magnitude as the other sensor signals. The scale factor is calculated to be 2449 and the error matrix is

$$E = \begin{bmatrix} 0.062 & -0.029 & 0.067 & -0.142 & 0.110 & 0.068 & 0.110 & -0.189 \\ 0.107 & 0.102 & -0.021 & 0.096 & -0.028 & 0.090 & -0.013 & 0.007 \\ 0.119 & 0.033 & 0.028 & -0.144 & 0.078 & -0.050 & -0.016 & -0.134 \\ 0.291 & -0.932 & 0.904 & -1.028 & 1.287 & 0.181 & 0.006 & -1.502 \end{bmatrix}$$

The failure is identified as sensor 4. The large shift in the ERA eigenvalues classifies the failure correctly as a random output failure. The large error made in the calculation of the scale factor indicates that the FDI algorithm may encounter difficulties when the failed sensor output rms level is of the same order of magnitude as the true sensor signals.

In experiment 5, the third sensor outputs a sine wave with frequency 1 rad/s. The frequency of the sine wave is identified by the ERA algorithm as a mode of vibration, along with the first, third, and fourth actual structural modes of vibration. The scale factor is calculated to be 0.6773 and the error matrix is given as

$$E = \begin{bmatrix} -0.030 & -0.020 & 0.005 & 0.018 & -0.002 & 0.008 & 0.146 & -0.020 \\ -0.053 & -0.024 & 0.025 & -0.002 & -0.021 & 0.017 & 0.024 & 0.109 \\ -0.009 & -0.055 & -0.031 & -0.078 & -0.054 & -0.015 & 0.022 & -0.033 \\ -0.031 & -0.041 & -0.018 & 0.002 & -0.008 & 0.017 & -0.011 & -0.046 \end{bmatrix}$$

Inspecting Table 2, it is seen that three of the failure criteria indicate sensor 3 as failing, whereas three indicate sensor 1. However, the cumulative indicator indicates sensor 3. Thus, sensor 3 is flagged as having failed, but is classified as a random failure due to the shift in the ERA identified eigenvalues. However, by inspecting the eigenvalues, the presence of an identified undamped eigenvalue at 1 rad/s would seem to indicate that the failed sensor is outputting a pure harmonic signal.

In experiment 6, the second sensor outputs a random signal whose rms magnitude is much smaller than the other signals. This represents the case of a sensor with zero output corrupted with noise. The scale factor is identified as 3.2857 and the error matrix for this case is

$$E = \begin{bmatrix} -0.003 & -0.006 & 0.002 & 0.002 & 0.002 & -0.008 & -0.011 & -0.002 \\ 0.107 & 0.104 & -0.021 & 0.097 & -0.028 & 0.090 & -0.014 & 0.009 \\ -0.006 & -0.007 & 0.004 & 0.005 & -0.000 & 0.007 & 0.000 & 0.006 \\ -0.003 & -0.005 & -0.009 & 0.000 & -0.003 & -0.001 & -0.000 & 0.002 \end{bmatrix}$$

The failure criteria indicates correctly that sensor 2 has failed. However, the FDI algorithm in some sense incorrectly classifies the failure as a state correlated failure. This incorrect classification is due to the fact that the small random signal does not greatly influence the ERA identified eigenvalues, nor do the error or scale factor matrices indicate any other form of failure. In a certain sense, this is also a correct classification for this failure in that the constants of the second row of C_1 (not shown) multiplying the states are all close to zero as previously discussed.

In experiment 7, a gain error of 0.7 is introduced into the signal conditioning unit for sensor 3. The data is corrupted with 10% noise and the error matrix is given as

$$E = \begin{bmatrix} 0.007 & 0.012 & -0.004 & -0.005 & -0.005 & 0.003 & 0.008 & -0.005 \\ 0.019 & 0.015 & -0.002 & 0.011 & 0.001 & 0.016 & -0.001 & -0.010 \\ 0.041 & 0.055 & -0.020 & -0.021 & -0.016 & -0.030 & -0.007 & 0.004 \\ 0.010 & 0.012 & 0.014 & -0.002 & 0.014 & 0.002 & 0.003 & 0.008 \end{bmatrix}$$

The FDI algorithm indicates sensor 3 has failed. The failure is classified as a gain error because the row in the scale factor matrix corresponding to the failed sensor has a standard deviation which is less than 10% of its mean value. In other words, the numbers comprising the third row are all close to one another.

In experiment 8, a correlated sensor failure is simulated for sensor 1. The correlated sensor failure output is given by

$$y_{lf} = [0.1\ 0.2\ 0.3\ 0.4\ 0.0\ 0.0\ 0.0\ 0.0]y_n + \text{noise}$$

where y_n is the nominal sensor outputs, and y_{lf} is the output of the first sensor in the failed mode. The scale factor is identified as 1.1365 and the error matrix is given as

$$E=\begin{bmatrix} -0.095 & -0.025 & 0.058 & -0.143 & -0.083 & 0.146 & 0.348 & 0.129 \\ 0.039 & 0.032 & 0.015 & 0.017 & 0.017 & 0.051 & 0.036 & 0.007 \\ 0.041 & 0.051 & 0.008 & -0.015 & -0.035 & -0.026 & -0.024 & -0.022 \\ 0.025 & 0.029 & -0.032 & 0.016 & 0.039 & -0.014 & 0.008 & 0.002 \end{bmatrix}$$

The FDI algorithm flags sensor 1 as the failed sensor. Because none of the other sensor failure classifications are met, the FDI correctly classifies the failure as a state correlated failure.

B. Example 2: Cantilever Beam Experiment

To further illustrate the FDI method, experiments were conducted using a cantilevered beam with two accelerometers attached as shown in Fig. 2. The beam has length 0.84 m, mass per unit length of 2.364 kg/m, moment of inertia of 3.02e-09 m^4 and a Young's modulus of 70 GPa. The measured natural frequencies and damping ratios for the first three modes of vibration are $f_1=7.04$ HZ, $f_2=44.02$ Hz, $f_3=122.63$ Hz, $\zeta_1=4.41\%$, $\zeta_2=0.68\%$, and $\zeta_3=0.33\%$.

Four different experiments were conducted with the cantilevered beam. These experiments are summarized in Table 3. The sampling time for each experiment was 0.002 s. ERA analysis was applied using 100 time points of data. Data acquisition capabilities led to the constraint of only placing two sensors on the beam. Therefore, it is not possible to directly calculate the scale factor matrix, in that with only two sensors the most dissimilar row is not defined. At the same time, one would not want to include both sensors in the scale factor matrix calculation. Therefore, the scale factor was calculated with the sensor which was known to be good. Table 4 presents the results of the seven failure criteria.

Table 2 Summary of experiments/failure criteria

Experiment no.	$\bar{F}_1$	$\bar{F}_2$	$\bar{F}_3$	$\bar{F}_4$	$\bar{F}_5$	$\bar{F}_6$	$\bar{F}_7$	Failed sensor
3	**1.00**	**1.00**	**1.00**	**1.00**	**1.00**	**1.00**	**1.00**	1
	0.00	0.00	0.00	0.00	0.00	0.00	0.00	
	0.00	0.00	0.00	0.00	0.00	0.00	0.00	
	0.00	0.00	0.00	0.00	0.00	0.00	0.00	
4	0.13	0.07	0.12	0.12	0.06	0.12	0.11	4
	0.08	0.43	0.08	0.06	0.19	0.06	0.16	
	0.10	0.11	0.10	0.08	**1.00**	0.08	0.27	
	1.00	**1.00**	**1.00**	**1.00**	0.48	**1.00**	**1.00**	
5	0.84	0.41	**1.00**	**1.00**	0.04	**1.00**	0.79	3
	0.85	0.21	0.84	0.81	0.01	0.65	0.62	
	1.00	**1.00**	0.80	0.99	**1.00**	0.65	**1.00**	
	0.59	0.54	0.49	0.75	0.03	0.47	0.53	
6	0.08	0.07	0.08	0.10	0.04	0.10	0.09	2
	1.00	**1.00**	**1.00**	**1.00**	**1.00**	**1.00**	**1.00**	
	0.08	0.03	0.07	0.08	0.55	0.08	0.15	
	0.05	0.05	0.06	0.07	0.06	0.07	0.06	
7	0.26	0.20	0.23	0.31	0.20	0.28	0.29	3
	0.38	0.80	0.39	0.37	0.39	0.37	0.53	
	1.00	0.10	**1.00**	**1.00**	**1.00**	**1.00**	**1.00**	
	0.33	**1.00**	0.32	0.42	0.55	0.37	0.58	
8	**1.00**	**1.00**	**1.00**	**1.00**	**1.00**	**1.00**	**1.00**	1
	0.21	0.64	0.19	0.15	0.41	0.15	0.29	
	0.22	0.07	0.19	0.18	0.44	0.16	0.21	
	0.16	0.22	0.15	0.15	0.38	0.14	0.20	

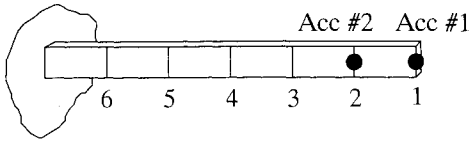

Fig. 2 Experimental beam.

The first experiment simulates a gain error in the first sensor. The gain was increased by a factor of 10. The scale factor was calculated to be -0.02, which is known to be incorrect from performing the experiment because the impulse was applied in the same direction. The error in the scale factor is attributed to a single large negative element in the scale factor matrix. If the element is ignored, the scale factor is calculated to be 0.68, which appears to be more reasonable. However, because an FDI algorithm should require no human intervention, the results listed use the -0.02 scale factor. The row norms of the nominal C matrix are 0.47 (row 1) and 0.30 (row 2). This is expected because sensor 1 is located at the tip of the cantilever beam. The row norms of the C matrix for experiment one are 1.32 (row 1) and 0.08 (row 2). One can obviously see the effect of using a poor scale factor. However, the gain difference can be seen by the relative magnitude difference between the two row norms. An approximation to the gain error can be calculated from

$$\text{gain error}=\left[\frac{\text{rnorm (row 1)}}{\text{rnorm (row 2)}}\right]_{\text{exp}}\Big/\left[\frac{\text{rnorm (row 1)}}{\text{rnorm (row 2)}}\right]_{\text{nom}} \quad (21)$$

where the subscripts exp and nom refer to the current experiment and nominal test case, respectively. Using Eq. (21), the gain error is approximated as 10.53. However, it should be noted that the scale factor matrix does not pass the standard deviation test for gain failure. Thus, the FDI algorithm classifies the failure as a state correlated failure.

The second experiment simulates a gain error in the second sensor. The gain was increased by a factor of 10. The scale factor is calculated to be 0.73. Again, the scale factor matrix does not pass the standard deviation test and the failure is classified as a state correlated failure.

Experiment 3 simulates a random signal error in the second sensor. The rms level of the random noise was of the same order of magnitude as the true signal (sensor 1). The scale factor was calculated to be 4.78, although it should be noted that one element of the scale factor matrix greatly increases the average. Because of the large eigenvalue shift in the fundamental frequency, the FDI algorithm classifies the failure as a random output.

Experiment 4 replaces accelerometer two with a broken accelerometer. The realized C matrix is calculated to be

$$C_1=\begin{bmatrix} 0.290 & 0.168 & -0.030 & -0.213 & -0.125 & -0.121 \\ -0.000 & -0.000 & -0.000 & 0.000 & -0.000 & -0.001 \end{bmatrix}$$

The failure is classified as a zero output failure because the row average of sensor 2 of the realized C matrix is -0.00028.

IV. Practical Implementation Issues

Although the motivation of this paper is to present the generic concept of system realization redundancy for FDI applications, the real-time capability of such algorithms must be addressed. However, such an analysis is difficult to assess in general terms. System specifics such as number of sensors, anticipated noise level of sensors, structure modal complexity, real-time computing power, how quickly failures must be detected, structural model knowledge, and other factors would define whether a given FDI algorithm is applicable. In the following, we address these issues in context with the proposed algorithm in more general terms.

The major computational burden imposed by the ERA based FDI algorithm is the singular value decomposition (SVD) of the $r\times p$ Hankel matrix, where $r=n1*1$ and $p=nm*m$. In defining r and p, 1 is the number of sensors, m the number of excitation sources used, nm the number of

Table 3 Summary of cantilever beam experiments

Experiment no.	ERA natural frequencies, Hz	Failure type	Failure detected
Nominal	7.04 44.02 122.63	—	—
1	7.04 44.03 122.66	Gain error (10) Sensor 1	State correlated Sensor 1
2	7.04 44.03 122.64	Gain error (10) Sensor 2	State correlated Sensor 2
3	11.90 44.12 122.50	Random signal Sensor 2	Random signal Sensor 2
4	7.05 44.00 122.58	No output Sensor 2	No output Sensor 2

Table 4 Summary of cantilever beam experiments/failure criteria

Experiment no.	$\bar{F}_1$	$\bar{F}_2$	$\bar{F}_3$	$\bar{F}_4$	$\bar{F}_5$	$\bar{F}_6$	$\bar{F}_7$	Failed sensor
1	**1.00**	**1.00**	**1.00**	**1.00**	**1.00**	**1.00**	**1.00**	1
	0.06	0.09	0.06	0.09	0.02	0.09	0.07	
2	0.16	0.39	0.17	0.10	**1.00**	0.11	0.34	2
	1.00	**1.00**	**1.00**	**1.00**	0.63	**1.00**	**1.00**	
3	**1.00**	0.14	**1.00**	0.83	0.59	0.84	0.78	2
	0.74	**1.00**	0.78	**1.00**	**1.00**	**1.00**	**1.00**	
4	0.55	0.25	0.72	0.34	**1.00**	0.47	0.55	2
	1.00	**1.00**	**1.00**	**1.00**	0.99	**1.00**	**1.00**	

data points per sensor used, and $n1$ the number of sample shifts used in forming the Hankel matrix. In typical applications, $r<p$ (Ref. 28). The flop count of the singular value decomposition using the Golub-Reinsch algorithm is $(2p^2r + 4pr^2 + 14r^3/3)$ (Ref. 29).

As with most FDI algorithms, increasing the number of sensors (1) will increase the computational burden. Assuming that the number of sensors is fixed, the value of r is dependent only on the number of sample shifts. It is known that both r and p must be greater than twice the number of structural modes that are desired to be identified. However, in the FDI application, it is not necessary to identify all the structural modes, but only a fixed number of modes which is system specific. In addition, it is possible to tradeoff identification accuracy (FDI sensitivity) vs computational burden. Thus, decreasing $n1$ will decrease the computational burden with a corresponding decrease in FDI sensitivity.

The column dimension of the Hankel matrix is dependent on the number of excitation sources and the number of time data points used from each sensor. In general, accuracy of the identified model is improved as p is increased. Increasing m aids the ERA algorithm in discerning closely spaced modes of vibration. However, from the FDI perspective, this may not be necessary so reducing m seems to be one way of improving the computational efficiency of the algorithm. This is especially true if a few excitation sources can adequately excite all sensors. Increasing the number of data points per sensor (nm) causes an increase in computational burden and an increase in the FDI data acquisition time but, in general, increases the robustness of the ERA algorithm to sensor noise. Thus, the selection of nm represents a complex tradeoff which can only be evaluated on a case-by-case basis. It should be noted that the ERA-DC algorithm[23] uses a data-correlated Hankel matrix of dimension $r \times r$, thus reducing the computational burden of the SVD (assuming $r<p$) to $32r^3/3$ flops. However, this reduction requires the matrix multiplication of the Hankel matrix and its transpose (HH^T).

It should be noted that although the tradeoffs associated with a FDI algorithm using realization based redundancy are different than analytical based redundancy systems, the general performance trends are similar. Analytical based systems using more time data will in general have better FDI capabilities. In addition, increasing the state-space dimension of the filter (either detection, Kalman, or Luenberg) and the number of filters will, in general, enhance the FDI algorithm performance.

The realization based FDI algorithm offers infinite robustness to modeling error by definition because no a priori model is required. However, it is important to guard against the case that a structural failure could be misinterpreted as a sensor failure. A major structural failure would cause a change in the identified state matrix A, which in turn would result in a change in the ERA identified eigenvalues and eigenvectors. Thus, it would be possible for the FDI algorithm to identify a failed sensor and classify it as a random failure when the actual cause was a structural failure. There are two checks that could be performed to guard against this misinterpretation. First, Eq. (10) could be utilized to compare the nominal state matrix (A_n) with the current and transformed state matrix ($T^{-1}A_1T$). A second check would be to immediately apply the FDI algorithm on the same data again, but this time removing the data associated with the identified "failed" sensor. If the realized eigenvalues are essentially the same as the nominal eigenvalues, then a correct sensor detection decision has been made. However, if the eigenvalues are the same, with and without the failed sensor, then this would indicate that the sensor did not corrupt the eigenvalue identification, and thus something else (i.e., the structural change) has caused the failure. If the identified eigenvalues do not fit in either category, then it is possible that multiple sensors have failed (as discussed previously) or that simultaneous structure and sensor failure has occurred.

V. Summary

A sensor failure detection and isolation algorithm has been presented which utilizes system realization theory. Instead of using hardware or analytical model redundancy, system realization is utilized to provide an experimental model based redundancy. The failure detection and isolation algorithm utilizes the eigensystem realization algorithm to determine a minimum-order state-space realization of the structure in the presence of noisy measurements. The failure detection and isolation algorithm then compares successive realizations to detect and isolate the failed sensor component. Because of the nature in which the failure detection and isolation algorithm is formulated, it is also possible to classify the failure mode of the sensor.

The algorithm has been demonstrated to perform well in the presence of noise. Some difficulties have been encountered when the rms output of the failed sensor is of the same order of magnitude as the rms outputs of the other sensors.

Acknowledgments

The authors greatly appreciate the support received from the Florida Space Grant Consortium Interinstitutional Space Research Program. In addition, the work of the second author was partially supported by a Harris Fellowship. The experimental equipment used in this research was obtained under NSF Grant MSM-8806869, grant monitor E. Marsh. The authors would also like to thank Jer-Nan Juang, L. Horta, and E. Garcia for discussions concerning the eigensystem realization algorithm.

References

[1]Willsky, A. S., "A Survey of Design Methods for Failure Detection in Dynamic Systems," *Automatica*, Vol. 12, Nov. 1976, pp. 601–611.

[2]Gertler, J. J., "Survey of Model-Based Failure Detection and Isolation in Complex Plants," *IEEE Control Systems Magazine,* Vol. 8, No. 6, 1988, pp. 3–11.

[3]Watanabe, K., and Himmelblau, D. M., "Fault Diagnosis in Nonlinear Chemical Processes," *American Institute of Chemical Engineering Journal,* Vol. 29, No. 2, 1983, pp. 243–249.

[4]Shiozaki, J., Matsuyama, H., Tano, K., and O'Shima, E., "Fault Diagnosis of Chemical Processes by the use of Signed, Directed Graphs: Extension to Five-Range Patterns of Abnormality," *International Chemical Engineering*, Vol. 25, No. 4, 1985, pp. 651–659.

[5]Kerr, T. H., "Decentralized Filtering and Redundancy Management for Multisensor Navigation," *IEEE Transactions on Aerospace and Electronic Systems,* Vol. AES-23, No. 1, 1987, pp. 83–119.

[6]Deckert, J. C., Desai, M. N., Deyst, J. J., and Willsky, A. S., "F8 DFBW Sensor Failure Identification Using Analytical Redundancy," *IEEE Transactions on Automatic Control,* Vol. AC-22, Oct. 1977, pp. 795–803.

[7]Baruh, H., and Choe, K., "Sensor Failure Detection Method for Flexible Structures," *Journal of Guidance, Control, and Dynamics,* Vol. 10, No. 5, 1987, pp. 474–482.

[8]VanderVelde, W. E., "Component Failure Detection in Flexible Spacecraft Control Systems," *Proceedings of the Fourth VPI & SU Symposium on Dynamics and Control of Large Flexible Structures,* May 1983, pp. 481–497.

[9]Beard, R. V., "Failure Accommodation in Linear Systems Through Self-Reorganization," Man Vehicle Laboratory, Rept. MVT-71-1, Cambridge, MA, 1971.

[10]Mehra, R. K., and Peschon, J., "An Innovations Approach to Fault Detection and Diagnosis in Dynamic Systems," *Automatica,* Vol. 7, No. 5, 1971, pp. 637–640.

[11]Montgomery, R. C., and Caglayan, A. K., "Failure Accommodation in Digital Flight Control Systems by Bayesian Decision Theory," *Journal of Aircraft*, Vol. 13, No. 2, 1976, pp. 69–75.

[12]Daly, K. C., Gai, E., and Harrison, J. V., "Generalized Likelihood Test for FDI in Redundant Sensor Configurations," *Journal of Guidance, Control, and Dynamics,* Vol. 2, No. 1, 1979, pp. 9–17.

[13]Clark, R. N., "Instrument Fault Detection," *IEEE Transactions on Aerospace and Electronic Systems,* Vol. AES-14, No. 3, 1978, pp. 456–465.

[14]Clark, R. N., and Campbell, B., "Instrument Fault Detection in a Pressurized Water Reactor Pressurizer," *Journal on Nuclear Technology,* Vol. 56, Jan. 1982, pp. 23–32.

[15]Frank, P. M., and Keller, L., "Sensitivity Discriminating Observer Design for Instrument Failure Detection," *IEEE Transactions on Aerospace and Electronic Systems,* Vol. AES-16, No. 4, 1980, pp. 460–467.

[16]Belkoura, M., "Entdeckung von Instrumentenfehlern mittels Kalman-Filter," Ph.D. Thesis, University of Duisburg, Germany, 1983.

[17]Frank, P. M., and Keller, L., "Entdeckung von Instrumentenfehlanzeigen mittels zustandsschatzung in technischen Regelungssystemen," *Fortschrittberichte,* VDI-Z, Reihe 8, 1984.

[18]Chow, E. Y., and Willsky, A. S., "Analytical Redundancy and the Design of Robust Failure Detection Systems," *IEEE Transactions on Automatic Control,* Vol. AC-29, No. 7, 1984, pp. 603–614.

[19]Lou, X. C., Willsky, A. S., and Verghese, G. L., "Optimally Robust Redundancy Relations for Failure Detection in Uncertain Systems," *Automatica,* Vol. 22, No. 3, 1986, pp. 333–344.

[20]Juang, J. N., and Pappa, R. S., "An Eigensystem Realization Algorithm (ERA) for Modal Parameter Identification and Model Reduction," *Journal of Guidance, Control, and Dynamics,* Vol. 8, No. 5, 1985, pp. 620–627.

[21]Kalman, R. E., "On Minimal Partial Realizations of a Linear Input/Output Map," *Aspects of Network and System Theory,* edited by R. E. Kalman and N. DeClaris, Holt, Rinehart, and Winston, New York, 1971, pp. 385–407.

[22]Juang, J.-N., "Mathematical Correlation of Modal Parameter Identification Methods Via System Realization Theory," NASA TM 87720, April 1986.

[23]Juang, J.-N., Cooper, J. E., and Wright, J. R., "An Eigensystem Realization Algorithm Using Data Correlations (ERA/DC) for Modal Parameter Identification," *Control Theory and Advanced Technology,* Vol. 4, No. 1, 1988, pp. 5–14.

[24]King, A. M., Desai, U. B., and Skelton, R. E., "A Generalized Approach to Q-Markov Covariance Equivalent Realization of Discrete Systems," *Automatica,* Vol. 24, No. 4, 1988, pp. 507–515.

[25]Moonen, M., DeMoor, B., Vandenberghe, L., and Vanderwalle, J., "On- and Off-Line Identification of Linear State-Space Models," *International Journal of Control,* Vol. 49, No. 1, 1989, pp. 219–232.

[26]Lew, J.-S., Juang, J.-N., and Longman, R. W., "Comparison of Several System Identification Methods for Flexible Structures," *Proceedings of the AIAA/ASME/ASCE/AHS/ASC 32nd Structures, Structural Dynamics and Materials Conference* (Baltimore, MD), AIAA, Washington, DC, 1991, pp. 2304–2318.

[27]Kailath, T., *Linear Systems,* Prentice-Hall, Englewood Cliffs, NJ, 1980.

[28]Juang, J.-N., private communication, 1991.

[29]Golub, G. H., and Van Loan, C. F., *Matrix Computations,* Johns Hopkins University Press, Baltimore, MD, 4th Printing, 1985, p. 175.